Catalysis Today 180 (2012) 124–130

Contents lists available at ScienceDirect

Catalysis Today

journal homepage: www.elsevier.com/locate/cattod

The influence of ceria and other rare earth promoters on palladium-based methane combustion catalysts

Sara Colussi [a], Alessandro Trovarelli [a,*], Cinzia Cristiani [b], Luca Lietti [c], Gianpiero Groppi [c]

[a] Dipartimento di Chimica, Fisica e Ambiente, Università di Udine, via del Cotonificio 108, 33100 Udine, Italy
[b] Dipartimento di Chimica, Materiali e Ingegneria Chimica "G. Natta", Politecnico di Milano, P.zza L. da Vinci 32, 20133 Milano, Italy
[c] Dipartimento di Energia, Laboratory of Catalysis and Catalytic Processes and NEMAS, Centre of Excellence, Politecnico di Milano, P.zza L. da Vinci 32, 20133 Milano, Italy

ARTICLE INFO

Article history:
Received 17 December 2010
Received in revised form 25 February 2011
Accepted 6 March 2011
Available online 27 April 2011

Keywords:
Ceria
Palladium
Catalytic combustion
Rare earths

ABSTRACT

In this work we investigate the effect of ceria and other rare earths (La, Pr, Tb) on Pd–PdO transformation, which is strongly related to the catalytic activity of Pd-based catalysts for the combustion of methane at high temperature. Also the behavior of Pd on ZrO_2 and on yttria-stabilized zirconia is considered for comparison. The catalysts are characterized by XRD and BET surface area measurements. Pd–PdO transformation is studied by means of temperature programmed oxidation measurements and thermogravimetric analysis. Temperature programmed combustion experiments have been carried out in order to compare catalytic activity of different catalysts. The results show that rare earth oxides promote the onset of Pd re-oxidation upon cooling, that for ceria doped sample is reflected in an improvement in the catalytic activity.

1. Introduction

High temperature catalytic combustion (HTCC) of methane has been widely studied as a valid alternative to conventional flame combustion for gas turbines applications [1–4]. Catalytic combustion allows to achieve low pollutants emissions (NO_x, CO and UHC) [5,6] and high combustion efficiency. Among all catalysts tested for HTCC of methane, PdO has been recognized to be the most active [7–9]. Palladium oxide though shows a particular redox behavior with a pronounced hysteresis between PdO reduction and Pd re-oxidation, observed, respectively, in the heating and in the cooling ramps of a thermal cycle. This peculiarity can affect negatively catalyst performance, causing a loss in methane conversion during the cooling part of combustion cycle [7,10,11].

The redox behavior of PdO has been the object of many investigations. Farrauto et al. [7] first studied Pd–PdO transformation by thermogravimetric analysis and found that PdO decomposition occurs in two steps, attributed to PdO dispersed on bulk palladium metal and to crystalline palladium oxide. In a subsequent work they investigated also the influence of different supports [12], finding that the hysteresis is strongly dependent on the support. They observed the largest hysteresis for ZrO_2-supported PdO, while TiO_2 and CeO_2 increase significantly the temperature of Pd re-oxidation during cooling, thus having small hysteresis effects. McCarty [13] and Groppi et al. [11] also individuated two decomposition peaks, corresponding to two PdO species. According to McCarty these species belong to bulk PdO and to a more stable surface or near surface oxide that decomposes at higher temperature. Groppi suggests that the two PdO species have a similar degree of oxidation excluding the presence of substoichiometric oxides and hypothesizes that the first PdO (the one that decomposes at lower temperature) corresponds to PdO in boundary contact with metallic Pd. Datye et al. [14] studied the microstructure of alumina-supported PdO during Pd–PdO transformation suggesting that the hysteresis in Pd re-oxidation upon cooling depends on a kinetic limitation instead of a thermodynamic one. In particular they did not observe any PdO even after holding the sample far below the temperature at which its formation would have been thermodynamically favored. Some authors studied also the effect of different supports and dopants on the catalytic performances of palladium-based catalysts. For example Rodriguez et al. [15] compared the behavior of palladium particles supported on γ-Al_2O_3, SiO_2 and ZrO_2, while Widjaja et al. [16] studied the effect of the addition on alumina of several oxides, among which the best resulted to be Co_3O_4 and NiO. Thevenin et al. [17] investigated catalytic activity and redox behavior of palladium catalysts supported on Ba- and La-stabilized alumina. In another work they observed that the addition of Ce increases Pd re-oxidation temperature [18]. More recently, our group characterized the structure and morphology of PdO supported on alumina and on ceria-doped alumina [19]. We observed that the effect of ceria is more important on Pd re-oxidation: in the cooling ramp of a thermal cycle Pd particles in contact with CeO_2

* Corresponding author.
E-mail address: trovarelli@uniud.it (A. Trovarelli).

0920-5861/$ – see front matter © 2011 Elsevier B.V. All rights reserved.
doi:10.1016/j.cattod.2011.03.021

are re-oxidized at higher temperature with respect to Pd particles in contact with bare alumina. From the comparison of TPO, HRTEM and XPS data we concluded that, while the onset of PdO decomposition is clearly dependant only on thermodynamics, Pd re-oxidation is a more complex phenomenon that involves kinetic limitations.

The present study is focused on the examination of Pd–PdO redox behavior on different supports (Al_2O_3 and ZrO_2) promoted with rare earths on alumina and yttria on zirconia. The goal of this work is to define the role of different supports and dopants on Pd–PdO transformation and to give some insights into palladium oxide redox behavior using different experimental techniques.

2. Experimental

2.1. Catalysts preparation

Alumina-supported samples were prepared by incipient wetness technique through impregnation of γ-Al_2O_3, LaRoche Versal TD250 (BET surface area 233 m^2/g after calcinaton at 1073 K for 6 h) with a solution of rare earth nitrates ($Ce(NO_3)_3{\cdot}6H_2O$, $La(NO_3)_3{\cdot}6H_2O$, Aldrich 99.99%, $Pr(NO_3)_3{\cdot}6H_2O$ and $Tb(NO_3)_3{\cdot}5H_2O$, Aldrich 99.9%). The nominal rare earth oxides (REO) loading was of 15 wt.% (REO = La_2O_3, PrO_x, TbO_x and CeO_2). After impregnation the samples were dried overnight at 393 K and calcined at 1273 K for 6 h. Doped supports were subsequently impregnated with a solution of 10 wt.% of $Pd(NO_3)_2$ (Aldrich, 99.999%), dried at 393 K overnight and calcined at 1073 K for 6 h, to obtain a catalyst with a nominal Pd loading of 10 wt.%. Undoped catalyst (10%Pd/Al_2O_3) was prepared also by incipient wetness impregnation with the same $Pd(NO_3)_2$ solution, dried overnight at 393 K and calcined at 1073 K for 6 h.

Zirconia based supports, ZrO_2 (XZO881/4) and YSZ (8% Y_2O_3, XZO 1012/01) provided by MEL Chemicals, were calcined in flowing air for 10 h at 1223 K (heating/cooling rate 2 K/min). The catalysts (nominal Pd loading of 10 wt.%) were prepared by incipient wetness technique on these supports using a commercial $Pd(NO_3)_2$ solution (Pd 12–16% (w/w), Alfa Aesar). The powders were dried at 383 K for 2 h and then calcined in flowing air at 873 K for 10 h.

2.2. Catalysts characterization

Surface area measurements were carried out with a Sorptomatic 1990 porosimeter by adsorption/desorption of nitrogen. Prior to adsorption measurements, samples were degassed for 2 h at 423 K.

Catalysts were characterized also by XRPD analysis. For the alumina-supported samples X-Ray spectra were collected with a Philips X'Pert diffractometer, while for zirconia samples spectra were collected with a PHILIPS PW 1050-70 diffractometer, both equipped with Cu Kα radiation. Catalytic powders were analyzed by Rietveld refinements of the XRPD data using the GSAS software package to attain structural information and quantitative phase composition [20].

Thermogravimetric analysis was carried out in order to evaluate the weight loss due to PdO reduction and the weight gain associated with PdO reformation, on a SEIKO TG/DTA 6300 instrument equipped with an EXSTAR 6000 interface. The samples were exposed to 10 vol.%. O_2 in N_2 while the temperature was raised up to 1273 K at a ramp of 10 K/min and then cooled down to room temperature at the same rate. For each sample three temperature cycles have been performed.

The effect of different supports and dopants on Pd–PdO transformation was investigated with temperature programmed oxidation (TPO) experiments performed in a quartz reactor (i.d. 4 mm, *l* 450 mm). The catalysts (50 μm < Ø < 100 μm) were loaded in the reactor on a quartz wool bed. In a typical TPO experiment the sample was exposed to 1 vol.% O_2 in He (total flowrate of 35 ml/min), heated up to 1273 K at a heating rate of 10 K/min, then cooled down to 473 K at 10 K/min before a new cycle started. For each catalyst six TPO cycles were performed and for all of them the reacting mixture was 1 vol.% O_2 in He. Measurements were carried out with an on-line Balzers QMG 420 quadrupole mass spectrometer and with an Agilent P200 micro-gaschromatograph for quantitative analysis.

Table 1
Nominal composition and BET surface area of the samples used in this work.

Sample	Composition (wt.%)	BET surface area (m^2/g)	BET surface area (m^2/g Al_2O_3)
Al_2O_3	–	148	148
PdAl	10%Pd/Al_2O_3	124	138
LaAl	15%La_2O_3/Al_2O_3	137	161
PdLaAl	10%Pd/15%La_2O_3/Al_2O_3	115	153
PrAl	15%Pr_6O_{11}/Al_2O_3	123	145
PdPrAl	10%Pd/15%Pr_6O_{11}/Al_2O_3	116	155
TbAl	15%Tb_4O_7/Al_2O_3	135	160
PdTbAl	10%Pd/15%Tb_4O_7/Al_2O_3	125	167
CeAl	15%CeO_2/Al_2O_3	123	145
PdCeAl	10%Pd/15%CeO_2/Al_2O_3	110	147
ZrO_2	–	15	–
PdZr	10%Pd/ZrO_2	14	–
YSZ	8%Y_2O_3/ZrO_2	10	–
PdYSZ	10%Pd/YSZ	9	–

2.3. TPC experiments

Temperature programmed combustion (TPC) experiments were carried out in a quartz tubular reactor (i.d. 6 mm, *l* 300 mm) in a fuel lean mixture (0.5 vol.% CH_4, 2 vol.% O_2 in He) and with a gas hourly space velocity (GHSV) of 180,000 h^{-1}; total flowrate was 0.18 Nl/min. The gas apparatus consisted of three mass flow controllers which supplied reaction gases to the reactor; upstream of reactor a gas mixer was positioned in order to ensure complete gas mixing. 60 mg of the powdered catalyst (particle diameter 50 μm < Ø < 100 μm) were mixed with an equal amount of quartz beads of the same size and loaded in the reactor on a quartz-wool bed. Temperature was measured with a fixed K-type thermocouple placed in the catalyst bed. The sample was heated up to 1173 K at a heating rate of 10 K/min then cooled down at the same rate to room temperature for two combustion cycles. The data presented in this work correspond to the second cycle, in which the behavior of the samples is stabilized [21]. Combustion products profiles were monitored with an on-line mass spectrometer (Hiden Analytical) downstream of the reactor.

3. Results

3.1. Textural and structural characterization

The results of BET surface area measurements, also referred to 1 g of Al_2O_3 support are shown in Table 1. As expected, alumina-supported catalysts show a surface area about one order of magnitude higher than zirconia-supported ones. After calcination at 1073 K all alumina-supported samples show a similar surface area and the data referred to 1 g of Al_2O_3 confirm a stabilizing effect of rare earth promoters.

XRD patterns of doped and undoped alumina-supported samples are reported in Fig. 1, while Table 2 summarizes phase composition and crystallites dimensions derived from Rietveld analysis. All the samples mainly consist of transition alumina, namely θ-Al_2O_3 [JCPDS 35-121] (70–80 wt.%). Furthermore, in case of Ce-, La- and Pr-doped samples, well crystallized CeO_2 [JCPDS 4-539] ($d_{cryst.}$ = 13 nm), $PrAlO_3$ [JCPDS 29-0077] ($d_{cryst.}$ =35 nm) and

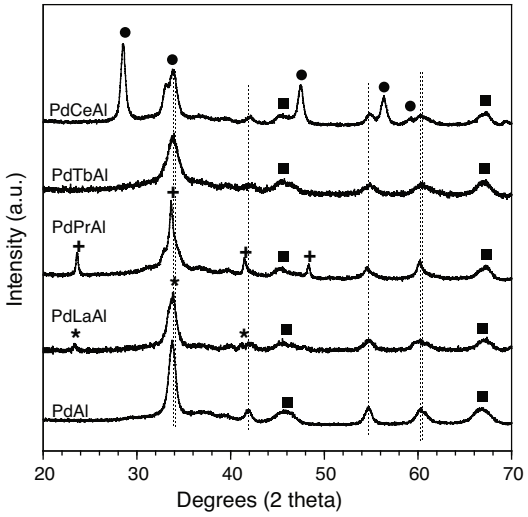

Fig. 1. XRD patterns of the alumina-supported samples calcined at 1073 K (■ = θ-alumina, * = $LaAlO_3$, + = $PrAlO_3$, ● = CeO_2, dotted bars = PdO).

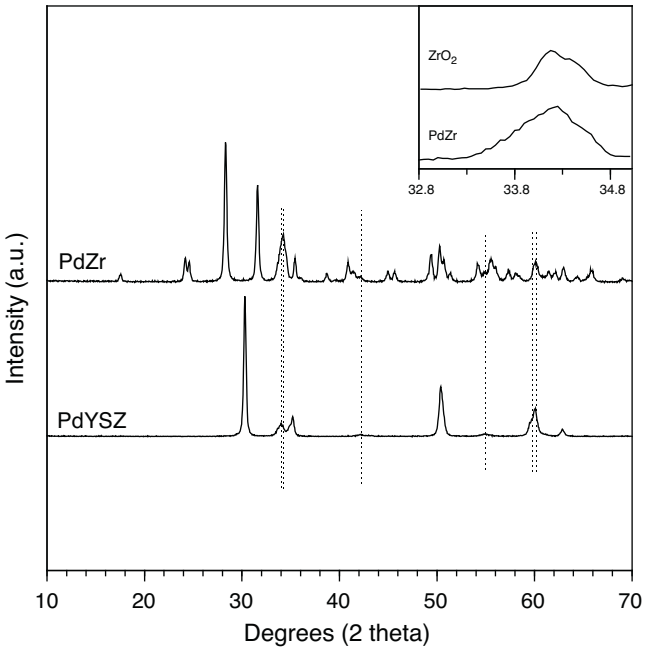

Fig. 2. XRD patterns of zirconia-supported samples (dotted bars = PdO, offset 32–34 2θ range).

$LaAlO_3$ [JCPDS 31-0022] ($d_{cryst.}$ =29 nm) phases are detected. Crystalline CeO_2, 14 wt.%, accounts for about the Ce total content while only small perovskite amounts are formed ($PrAlO_3$ = 3.5 wt.% and $LaAlO_3$ = 1 wt.%). The formation of some $PrAlO_3$ and $LaAlO_3$ indicates that Pr and La are present in the RE^{3+} form. For Tb-doped material the presence of crystalline $TbAlO_3$ was detected only in samples calcined at temperatures higher than 1273 K, even if TPR experiments showed that after calcination at 1273 K also Tb was present in the +3 state [22]. As a result Pr, Tb and La ions are thus highly dispersed on the support.

Only crystalline PdO [JCPDS 41-1107] is detected in all the samples, according to Liotta et al., where the presence of oxidized Pd-species are found on similar systems [23]. PdO crystallites are larger on pure Al_2O_3 than on RE-doped samples (10 and 5–9 nm, respectively). Apparently, Rietveld analysis slightly overestimates PdO content (Table 2). However, this result is due to both the low crystallinity of the main sample component, e.g. θ-Al_2O_3, that is hardly modeled by the calculation program and to the overlapping of the PdO reflections with the alumina ones. Accordingly, calculated PdO can be considered in reasonable agreement with the nominal content (10 wt.%), thus accounting for the total Pd content.

In Fig. 2 XRD patterns of zirconia-supported catalysts are reported. For PdZr sample monoclinic ZrO_2 is present [JCPDS 37-1484]. Because of the large overlapping of PdO reflection with M-ZrO_2 ones, PdO only can be qualitatively evidenced by the broadening of the peak at 2θ = 34.5 (offset in Fig. 2). In PdYSZ sample, a mixed tetragonal-cubic ZrO_2 phase is detected [24] and palladium ions are still present as PdO (11 wt.%) with crystallites larger than those found in alumina-based samples (15 nm vs 5–10 nm).

Table 2
Phase composition and crystallites dimensions of the samples as calculated from Rietveld analysis.

Sample	Phase composition (XRD)	Crystallite dimensions (nm)
PdAl	88%θ-Al_2O_3, 12%PdO	PdO = 10
PdLaAl	17%PdO, 82%θ-Al_2O_3, 1%$LaAlO_3$	PdO = 9 ($LaAlO_3$ = 29)
PdPrAl	14%PdO, 3.5%$PrAlO_3$, 82.5%θ-Al_2O_3	PdO = 5 ($PrAlO_3$ = 35)
PdTbAl	14%PdO, 86%θ-Al_2O_3	PdO = 5.5
PdCeAl	14% CeO_2, 12%PdO, 74%θ-Al_2O_3	PdO = 9 (CeO_2 = 13)
PdZr	90% M, 10%PdO	PdO = not measured (M = 49)
PdYSZ	89%T-C, 11%PdO	PdO = 15

3.2. Temperature programmed oxidation experiments

According to Rietveld analysis on fresh samples (see Table 2), for all catalysts Pd is present only in the oxide form before TPO experiments. TPO profiles on PdAl catalyst are shown in Fig. 3a. The first cycle is different from the others and this was detected for all samples, since it presents only one oxygen release peak at T = 1130 K. In the following cycles PdO decomposition takes place in three steps: a first decomposition peak at about 1000 K (whose intensity increases from cycle 1 to cycle 6), a second decomposition peak at about 1070 K with almost constant area and a third one (T = 1120 K) with decreasing intensity. This evolution is more evident in the first three cycles and is less pronounced from the fourth cycle on. During heating, also a broad oxygen uptake peak was observed, right before the beginning of the decomposition, from the second cycle onwards. In the cooling part of the TPO cycles only one oxygen uptake peak at about T = 750 K is detected, which does not significantly change cycle by cycle. The PdZr sample (Fig. 3b) shows a similar dynamic behavior during the heating ramp, but the decomposition takes place at slightly different temperatures: the first peak at about 1020 K, the second peak still at 1070 K and the third one at 1100 K. During cooling, re-oxidation takes place in one peak, as for the Al_2O_3 supported sample, but at higher temperature (T = 820 K).

In Fig. 4 the sixth TPO cycle is reported for all catalysts; this cycle has been chosen as the more representative since from cycle 5 onwards no further modification in Pd–PdO transformation is observed. PdO decomposition threshold does not depend on the support, in fact for all the samples it takes place almost at the same temperature, as reported in Table 3. The onset of PdO decomposition recorded for all these samples is well in agreement with the temperature of decomposition of bulk PdO under 1 vol.% O_2 partial pressure as calculated from [25], i.e. about 968 K. However, the addition of REO strongly affects the features of Pd–PdO transformation, and the effects are different when RE = Tb, Ce or Pr.

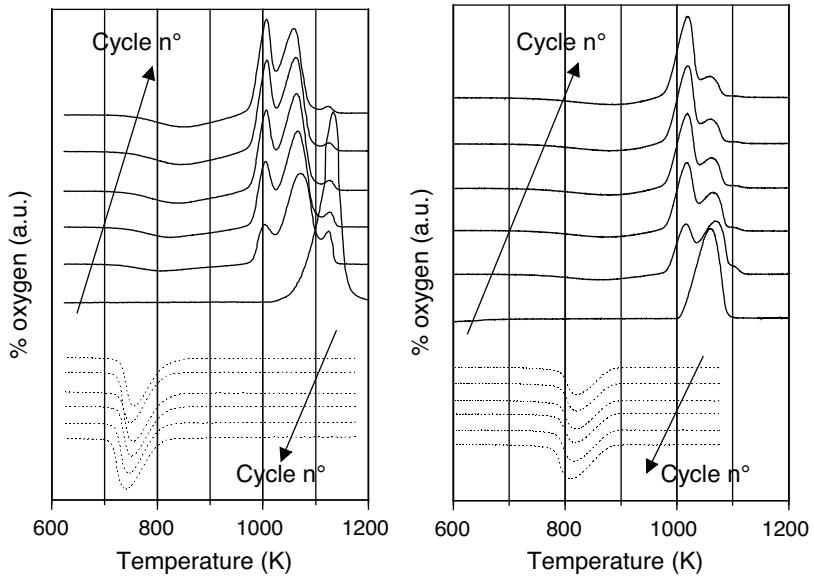

Fig. 3. (a) Oxygen uptake-release profile for six TPO cycles of PdAl sample (solid line = heating, dotted line = cooling). (b) Oxygen uptake-release profile for six TPO cycles of PdZr sample (solid line = heating, dotted line = cooling).

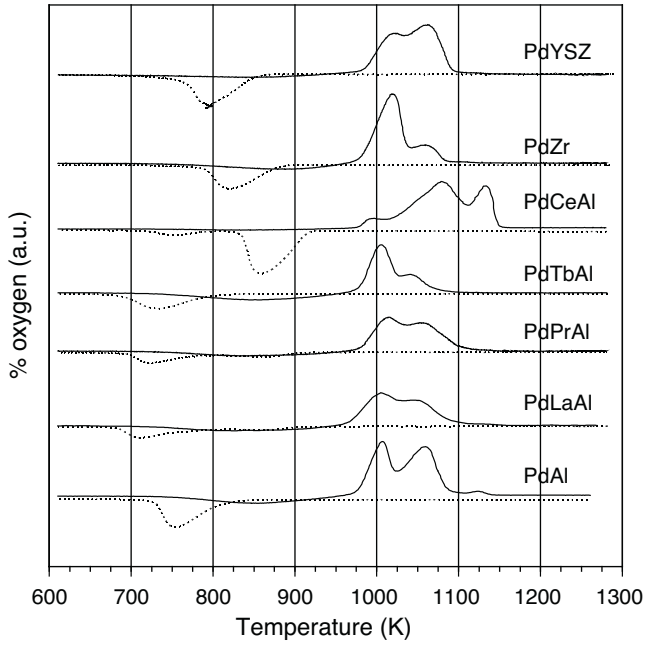

Fig. 4. Sixth TPO cycle for all the catalysts considered in this work (solid line = heating, dotted line = cooling).

PdCeAl sample shows the presence of three decomposition peaks, the first one at about 990 K, the second at $T = 1080$ K and the third at $T = 1140$ K. The decomposition temperatures are close to those of alumina-supported PdO, but there is great difference in the amount of oxygen released for each peak: CeO_2 strongly promotes high temperature decomposition stages. In the case of PdCeAl the intensities of the first and third peak are the opposite with respect to the same peaks of PdAl, while the dynamic behavior is the same (increasing of the first peak and decreasing of the third one during subsequent cycles).

The main difference between Al_2O_3 and CeAl-supported catalysts is in the cooling part of the cycle [18,26,27]. When CeO_2 is added as dopant, Pd re-oxidation takes place in two steps: a first oxygen uptake peak with maximum at $T = 860$ K, which is the more relevant, and a second, smaller oxygen uptake peak at $T = 750$ K. Moreover with CeO_2 the re-oxidation peak during heating almost disappears, as it can be inferred also from quantitative analysis reported in Table 3. Also in the samples containing 15%Pr or 15%La, which behave quite similarly, O_2 uptake during cooling is significantly anticipated with respect to the Al_2O_3 supported catalysts, but differently from the CeO_2 doped samples, no promotion of the re-oxidation extent during cooling is observed and a large fraction of the oxidation process occurs during the following heating ramp (see Table 3). When Tb is used as dopant inhibition of Pd re-oxidation is more evident. During the heating part of the cycle only two decomposition peaks can be detected for La-, Pr- and Tb-doped catalysts, at the same temperatures as the undoped sample ($T = 1000$ K and $T = 1050$ K).

Zirconia-based supports significantly anticipate re-oxidation upon cooling with respect to alumina-based supports (except CeAl) and slightly promote total re-oxidation. When ZrO_2 is stabilized with yttria, Pd re-oxidation is shifted to a lower temperature ($T = 790$ K); the presence of yttria enhances the oxidation extent as revealed by the larger high temperature decomposition peak and confirmed by quantitative analysis.

Table 3
Quantitative analysis and threshold temperatures for Pd–PdO transformation from TPO experiments.

Sample	PdAl	PdLaAl	PdPrAl	PdTbAl	PdCeAl	PdZr	PdYSZ
Decomposition threshold T (K)	970	965	978	968	977	975	980
Reoxidation threshold T (K)	840	910/813	913/800	848	918/800	895	870
O_2 release %	86	82	78	81	93	82	88
O_2 uptake % (cooling)	61	58	59	42	89	64	77
O_2 uptake % (heating)	22	27	21	39	6	21	8
Total O_2 uptake %	83	85	80	81	95	85	85

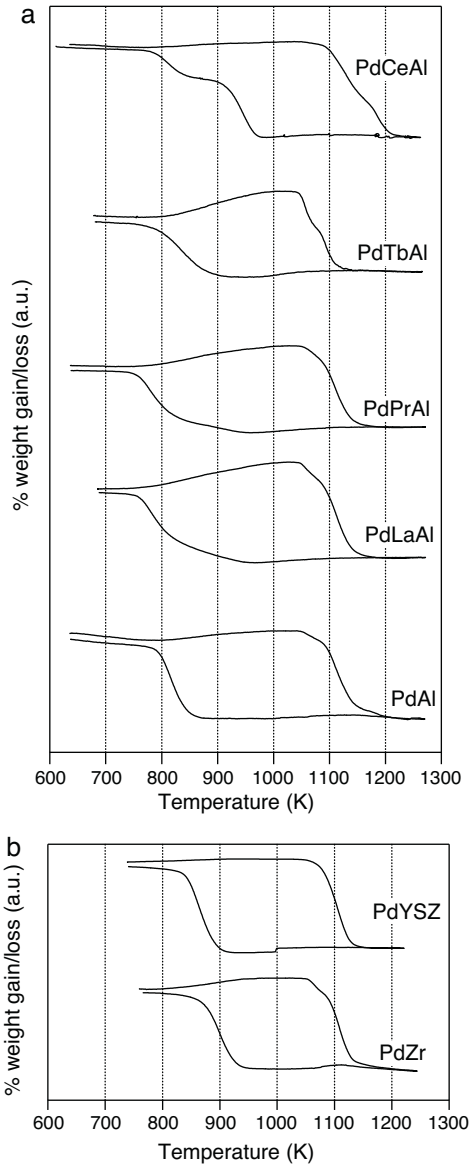

Fig. 5. (a) Thermogravimetric profiles of alumina-supported samples (10% O_2 in nitrogen). (b) Thermogravimetric profiles of zirconia-supported samples (10% O_2 in nitrogen).

3.3. Thermogravimetric analysis

In Fig. 5a and b the weight gain/loss during the third temperature cycle of thermogravimetric measurements are reported for alumina based and zirconia based samples, respectively. These experiments are complementary to the results obtained in the TPO cycles. For all the samples the threshold temperatures for both decomposition and re-oxidation are shifted to higher values than in TPO experiments due to the higher oxygen partial pressure (10% O_2 in N_2) [19]. Also in this case, the onset of PdO decomposition is in agreement with the temperature of decomposition of bulk PdO under 10 vol.% O_2 partial pressure (1048 K) [25]. In line with TPO results, any effect of the support can hardly be observed on the onset of PdO decomposition, however in the case of PdCeAl catalyst PdO decomposition is completed about 50 K above the other alumina-supported catalysts.

The two re-oxidation steps during cooling, observed also in TPO profiles, are clearly evident in the case of PdCeAl catalyst, the first one being markedly anticipated with respect to the catalyst supported onto undoped Al_2O_3. Ceria also strongly promotes the extent of Pd re-oxidation which is practically completed during the cooling ramp.

Regarding rare-earth promoted catalysts, it can be observed (see also Table 4) that the threshold for Pd re-oxidation (corresponding to a weight gain of the sample) is similar for PdLaAl and PdPrAl (about 950 K) and close to that of PdCeAl (~975 K). What is very different is the slope of the weight gain curve, which is significantly lower for lanthana and praseodymia doped samples, indicating a slower re-oxidation of the catalysts with respect to the ceria doped one. In particular, a two-slope trend is observed indicating that the oxidation process significantly accelerates upon reaching a critical extent. For PdTbAl re-oxidation threshold (about 915 K) is lower than on PdCeAl, but still significantly higher than on the undoped Al_2O_3 sample (~870 K). On the other hand, despite of the higher temperature, re-oxidation during cooling is slower over La-, Pr- and Tb-doped samples and proceeds to a large extent during the following heating ramp.

A positive effect of temperature on Pd re-oxidation rate is observed on samples supported onto zirconia based materials. For PdYSZ the threshold for Pd re-oxidation during cooling is very close to that observed for PdTbAl (915 K), while for PdZr it is a little bit higher (938 K) in agreement with what observed in TPO experiments (Table 3). For both samples the slope of the weight gain is quite steep indicating that Pd re-oxidation is fast. Nevertheless, particularly on PdZr, re-oxidation is not completed during cooling and proceeds further in the following heating ramp.

3.4. Temperature programmed combustion experiments

In Fig. 6a and b the cooling part of the light-off cycle for alumina-based and zirconia-based samples are shown, respectively. As reported in the literature all conversion curves show a pronounced minimum, which has been attributed to the activity of Pd metal, present at high temperature, which is lower than that of PdO, that is progressively formed on decreasing the temperature [7]. Along these lines it can be observed that the position of the minima in conversion is in agreement with the trend of re-oxidation thresholds reported during TPO and TG experiments. PdCeAl sample has the minimum at the highest temperature (about 920 K), while PdPrAl and PdLaAl show minima at about 900 K. The behavior of PdTbAl is similar to that of PdAl in this respect, even if their re-oxidation thresholds are different. Also the values for minima in conversion are similar: 28% for PdTbAl and 32% for PdAl. With La the minimum is close to that of PdAl (31%). When Ce is added to the support, the hysteresis due to the reduction of PdO to Pd is strongly reduced and the minimum conversion is 75%, far above the other alumina-supported samples.

Also for zirconia supported samples the temperatures at which the minima in methane conversion are reached are in agreement with the trend in re-oxidation thresholds: about 960 K for PdZr and about 930 K for PdYSZ. The minimum conversion value for PdZr is 76% and 51% for PdYSZ. The undoped sample is better than the yttria-doped one and is close to the behavior of the PdCeAl catalyst.

4. Discussion

BET surface area measurements of the alumina-supported catalysts indicate that globally the addition of the noble metal lowers the surface area of the samples. This effect is more pronounced with the addition of rare earth oxides with higher molecular weight than Pd. When looking at the data of the supports referred to 1 g of alumina instead of 1 g of sample, it can be observed that there is a slight stabilizing effect operated by RE promoters (as already observed in a previous work [22]), not so pronounced due to the low calcina-

Table 4
Quantitative analysis and threshold temperatures for Pd–PdO transformation from TGA experiments (10% O_2).

Sample	PdAl	PdLaAl	PdPrAl	PdTbAl	PdCeAl	PdZr	PdYSZ
Decomposition threshold T (K)	1049	1048	1050	1044	1050	1052	1053
Reoxidation threshold T (K)	868	955/830	953/835	911	974/850	938	914
O_2 release %	92	85	90	86	100	99	100
O_2 uptake % (cooling)	84	65	67	62	97	86	93
O_2 uptake % (heating)	9	18	21	25	2	13	3
Total O_2 uptake %	93	83	88	87	99	99	96

tion temperature. This stabilizing effect is more evident after the addition of the active phase.

The XRD analysis of the RE-promoted samples reveals that Ce is completely segregated as crystalline CeO_2, whereas other REO are well dispersed on the alumina support, only a small fraction of La and Pr being segregated as crystalline aluminate perovskites and Tb being completely amorphous. The experiments carried out on Pd-based catalysts on different supports show primarily that Pd–PdO transformation is strongly affected by the nature of the support itself and this has a great influence also on catalytic activity.

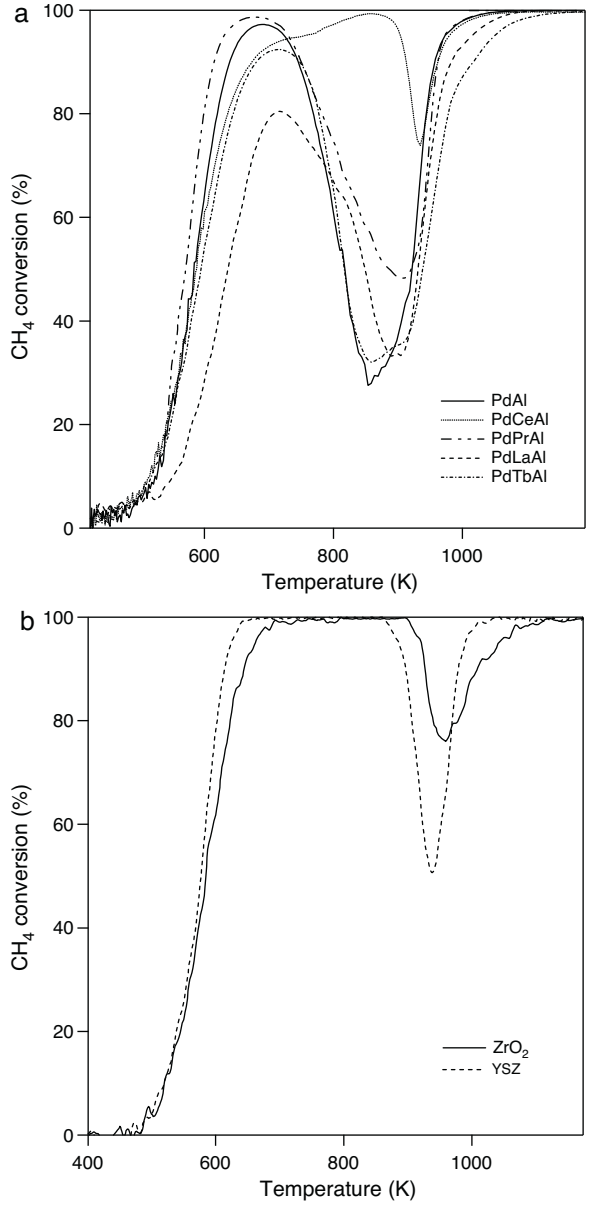

Fig. 6. (a) Cooling part of light-off curves for alumina-supported catalysts (0.5 vol.% CH_4, 2 vol.% O_2, He to balance). (b) Cooling part of light-off curves for zirconia-supported catalysts (0.5 vol.% CH_4, 2 vol.% O_2, He to balance).

Quantitative analysis based on TPO and TGA experiments (Tables 3 and 4) indicates that oxygen uptake upon cooling is higher for PdCeAl, PdYSZ and PdZr. The opposite is true for the oxygen uptake during heating. The total amount of oxygen uptake during TPO is similar for all catalysts with the exception of PdCeAl that has the higher oxygen uptake (10% more than the others). This is intimately related to the higher Pd oxidation extent in the ceria-containing support confirmed by quantitative analysis and inferred also from the observation of the TPO and TGA profiles (see Figs. 4 and 5a, b). From quantitative analysis of TGA experiments, carried out at a higher oxygen partial pressure (10% O_2), also PdZr and PdYSZ show the same oxygen uptake amount (see Table 4). TPO profiles indicate that ceria promotes high temperature decomposition stages of PdO associated with higher Pd oxidation extent. For PdYSZ, the intensity of high temperature decomposition peak and oxygen uptake during cooling are higher than PdZr. For all the other catalysts, the decomposition is completed at lower temperature with high temperature decomposition peaks that in general are smaller with respect to the ceria-doped catalyst. The nature of the support affects only the shape and the relative dimensions of the decomposition peaks, since the decomposition thresholds are quite similar for all catalysts, the main difference being of 15 K.

A completely different situation occurs for the re-oxidation threshold, which is strongly dependent on the nature of the support. Two re-oxidation steps are clearly observed for Ce-doped sample in both TPO and TGA profiles. For TPO the first one starts between 918 and 910 K and the second one between 813 and 800 K, while for TGA the temperatures are about 50 K higher due to the higher oxygen partial pressure. Also La- and Pr-doped catalysts show two re-oxidation steps, which are more evident in TGA profiles (Fig. 5a) where the weight gain curve presents two different slopes. The thresholds for these oxygen uptake stages are close to those of PdCeAl, nevertheless the oxidation is much slower and proceeds to a less extent with respect to Ce-doped sample (see also Tables 3 and 4 for quantitative analysis). This peculiar situation, in which the anticipated onset of Pd re-oxidation is not followed by a fast oxygen uptake, can be tentatively explained by a decoration effect of the promoters in disperse form (La, Pr and Tb) on palladium particles during TPO and TG cycles when Pd metal is present on catalyst surface [28]. Within this frame, La and Pr could promote the onset of re-oxidation at high temperature during the cooling ramp (as it happens for Ce) with the nucleation of small PdO clusters that have been reported to form before bulk PdO phase [29], but the decoration of Pd particles would significantly slow down the process that is even slower than on PdAl. Noteworthy once oxidation reaches a critical extent the slope of the TG profiles get steeper despite of lower temperature, possibly due to the reversibility of the decoration process under oxidizing conditions, as observed for Rh supported on La_2O_3 [30]. Re-oxidation is finally completed at high temperature (during the following heating ramp). For PdCeAl this does not happen, because CeO_2 is present in crystalline form, as evidenced by XRD analysis, and in this case a topological effect is predominant, i.e. Pd particles in contact with CeO_2 re-oxidize much

faster than other particles [27]. The behavior of PdTbAl is somehow different: it presents only one oxygen uptake feature in both TPO and TGA profiles, with threshold temperatures that are higher than PdAl but lower than other RE-promoted samples. Anyway also in this case Pd re-oxidation is completed at a lower temperature with respect to PdAl despite the anticipated threshold, suggesting again the possibility of a decoration effect on Pd particles.

Regarding zirconia-supported samples, a promotion of Pd oxidation is observed with respect to PdAl catalyst. The onset of Pd re-oxidation during cooling is anticipated, and re-oxidation occurs in a single step, although, particularly on PdZr, it is completed only in the following heating ramp possibly due to the larger particle size of Pd as revealed (at least for YSZ) by XRD analysis. Noteworthy, on PdYSZ Pd is oxidized at a higher extent during cooling than on PdZr (see Tables 3 and 4), even if the re-oxidation threshold is slightly lower. In this case oxygen mobility could be the determining step for the higher oxidation extent during cooling on PdYSZ, in agreement with what observed for PdCeAl. A transfer of oxygen from CeO_2 (and partly from YSZ) to PdO could take place at the Pd-CeO_2 boundary not exposed to the oxidizing atmosphere, in a way similar to that described for the oxidation of heavy hydrocarbon exhausts or for the oxidation of soot operated by ceria [31,32].

The thresholds of Pd re-oxidation are a very important factor and are reflected in the cooling part of the light-off curves, where the positions of the minima in methane conversion are strictly related to the onset temperatures for oxygen uptake during TPO experiments. This is true for both alumina and zirconia supports. On the other side, it is not easy to explain the different values for the minima on the different samples. One possible explanation could consider the contribution of two parameters: the first and most important is the onset of oxygen uptake, the second is the ease of re-oxidation, that is lower for La-, Pr- and Tb-doped samples for which we have hypothesized a decoration of Pd particles. PdCeAl and PdZr are the samples which have the higher temperatures for Pd re-oxidation, and accordingly show the lower loss in conversion.

5. Conclusions

Pd-based catalysts for the combustion of methane have been investigated. Catalytic activity upon cooling is strongly affected by Pd re-oxidation, which in turn is controlled by the nature of the support. The role of support on Pd re-oxidation is complex and involves both direct surface interaction, as for ceria-doped catalyst, and indirect control of Pd dispersion, as for Pd supported on zirconia.

All the dopants investigated in this work, and also bare zirconia support, promote the onset of Pd oxidation upon cooling with respect to PdAl, i.e. the nucleation of PdO clusters, but this promotion is not always followed by a fast oxidation. A fast Pd re-oxidation has been observed only for PdCeAl, and, to a less extent, for zirconia supported samples. The decoupling of onset and rate of re-oxidation has been tentatively ascribed to a decoration effect that can take place on La-, Pr- and Tb-doped samples. This effect can explain the significant inhibition of Pd oxidation observed on these samples. On PdLaAl, PdPrAl and PdTbAl Pd-reoxidation is completed only upon further heating, and the oxygen uptake amount during heating is higher than for PdCeAl.

These results are reflected on catalytic activity for methane combustion upon cooling. A high threshold for Pd re-oxidation can significantly improve catalytic activity during cooling, as observed for PdCeAl, PdZr and PdYSZ. Nevertheless, anticipated re-oxidation threshold is not enough to enhance catalytic activity, since also Pr, La and Tb anticipate Pd re-oxidation but their effect on activity loss is almost negligible.

Acknowledgment

This work has been financially supported by MIUR (Italy) under PRIN projects.

References

[1] T. Furuya, K. Sasaki, Y. Hanakata, T. Ohhashi, M. Yamada, T. Tsuchiya, Y. Furuse, Catal. Today 26 (1995) 345–350.
[2] P. Forzatti, Catal. Today 83 (2003) 3–18.
[3] S.A. Yashnik, N.V. Shikina, Z.R. Ismagilov, A.N. Zagoruiko, M.A. Kerzhentsev, V.N. Parmon, V.M. Zakharov, B.I. Braynin, O.N. Favorski, A.M. Gumerov, Catal. Today 147S (2009) S234–S243.
[4] R. Carroni, T. Griffin, Catal. Today 155 (2010) 2–12.
[5] P. Forzatti, G. Groppi, Catal. Today 54 (1999) 165–180.
[6] D. Ciuparu, M.R. Lyubovsky, E. Altman, L.D. Pfefferle, A. Datye, Catal. Rev. 44 (2002) 593–649.
[7] R.J. Farrauto, M.C. Hobson, T. Kennelly, E.M. Waterman, Appl. Catal. A 81 (1992) 227–237.
[8] R. Burch, F.J. Urbano, Appl. Catal. A 124 (1995) 121–138.
[9] O. Demoulin, M. Navez, P. Ruiz, Appl. Catal. A 295 (2005) 59–70.
[10] P. Salomonsson, S. Johansson, B. Kasemo, Catal. Lett. 33 (1995) 1–13.
[11] G. Groppi, G. Artioli, C. Cristiani, L. Lietti, P. Forzatti, Stud. Surf. Sci. Catal. 136 (2001) 345–350.
[12] R.J. Farrauto, J.K. Lampert, M.C. Hobson, E.M. Waterman, Appl. Catal. B 6 (1995) 263–327.
[13] J.G. McCarty, Catal. Today 26 (1995) 283–293.
[14] A.K. Datye, J. Bravo, T.R. Nelson, P. Atanasova, M. Lyubovsky, L. Pfefferle, Appl. Catal. A 198 (2000) 179–196.
[15] N.M. Rodriguez, S.G. Oh, R.A. Dalla-Betta, R.T.K. Baker, J. Catal. 157 (1995) 676–686.
[16] H. Widjaja, K. Sekizawa, K. Eguchi, H. Arai, Catal. Today 47 (1999) 95–101.
[17] P.O. Thevenin, E. Pocoroba, L.J. Pettersson, H. Karhu, I.J. Väyrynen, S.G. Järås, J. Catal. 207 (2002) 139–149.
[18] P.O Thevenin, A. Alcalde, L.J. Pettersson, S.G. Järås, J.L.G. Fierro, J. Catal. 215 (2003) 78–86.
[19] S. Colussi, A. Trovarelli, E. Vesselli, A. Baraldi, G. Comelli, G. Groppi, J. Llorca, Appl. Catal. A 390 (2010) 1–10.
[20] H.M. Rietveld, J. Appl. Crystallogr. 2 (1969) 65, using the program GSAS written by A.C. Larson and R.B. Von Dreele, "General Structure Analysis System", Los Alamos National Laboratory Report LA-UR-86-748, 2000.
[21] A. Baylet, S. Royer, P. Marécot, J.M. Tatibouët, D. Duprez, Appl. Catal. B 77 (2008) 237–247.
[22] S. Colussi, C. de Leitenburg, G. Dolcetti, A. Trovarelli, J. Alloys Compd. 374 (2004) 387–392.
[23] L.F. Liotta, G. Deganello, D. Sannino, M.C. Gaudino, P. Ciambelli, S. Gialanella, Appl. Catal. A 229 (2002) 217–227.
[24] R. Srinivasan, R.J. De Angelis, G. Ice, B.H. Davis, J. Mater. Res. 6 (1991) 1287–1292.
[25] J. Nell, St.F H., C. O'Neill, Geochim. Cosmochim. Acta 60 (1996) 2487–2493.
[26] G. Groppi, C. Cristiani, L. Lietti, C. Ramella, M. Valentini, P. Forzatti, Catal. Today 50 (1999) 399–412.
[27] S. Colussi, A. Trovarelli, G. Groppi, J. Llorca, Catal. Commun. 8 (2007) 1263–1266.
[28] S. Bernal, J.J. Calvino, C. López-Cartes, J.M. Pintado, J.A. Pérez-Omil, J.M. Rodríguez-Izquierdo, K. Hayek, G. Rupprechter, Catal. Today 52 (1999) 29–43.
[29] H. Gabasch, W. Unterberger, K. Hayek, B. Klötzer, E. Kleimenov, D. Teschner, S. Zafeiratos, M. Hävecker, A. Knop-Gericke, R. Schlögl, J. Han, F.H. Ribeiro, B. Aszalos-Kiss, T. Curtin, D. Zemlyanov, Surf. Sci. 600 (2006) 2980–2989.
[30] G.R. Gallaher, J.G. Goodwin Jr., L. Guczi, Appl. Catal. 73 (1991) 1–15.
[31] J.C. Fu, L. Czarnecki, C. Patellis, A. Bouney, W.A. Whittenberger, Proceedings of the Air Waste Management Association, 92nd Annual Meeting, St. Louis, USA, 1999, paper 99-217.
[32] E. Aneggi, M. Boaro, C. de Leitenburg, G. Dolcetti, A. Trovarelli, Catal. Today 112 (2006) 94–98.